www.czasopisma.pan.pl PAN POLSKA AKADEMIA NAUK www.journals.pan.pl

ARCHIVES OF ACOUSTICS
Arch. Acoust., **35**, 1, 91–109 (2010)

DOI: 10.2478/v10168-010-0007-3

Narrow Beam Ultrasonic Transducer Matrix Model for Projection Imaging of Biological Media

Krzysztof J. OPIELIŃSKI, Tadeusz GUDRA, Piotr PRUCHNICKI

Wrocław University of Technology
Institute of Telecommunications, Teleinformatics and Acoustics
Wybrzeże Wyspiańskiego 27, 50-370 Wrocław, Poland
e-mail: krzysztof.opielinski@pwr.wroc.pl

(*received July 4, 2009; accepted February 15, 2010*)

The following paper presents an idea of minimising the number of connections of individual piezoelectric transducers in a row-column multielement passive matrix system used for imaging of biological media structure by means of ultrasonic projection. It allows to achieve significant directivity with acceptable input impedance decrease. This concept was verified by designing a model of a passive ultrasonic matrix consisting of 16 elementary piezoceramic transducers, with electrode attachments optimised by means of electronic switches in rows and columns. Distributions of acoustic field generated by the constructed matrix model in water and results of the calculations conformed well.

Keywords: ultrasonic projection; directional ultrasonic transducer matrix; multielement ultrasonic probe; electrode attachment optimisation.

1. Introduction

The ongoing search for improved ultrasonic imaging performance will continue to introduce new challenges for beamforming design (Thomenius, 1996). The goal of the beamformer is to create a narrow and uniform beam with low sidelobes over a depth as long as possible. Among the already proposed imaging methods and techniques are: elevation focusing (1.25D, 1.5D and 1.75D arrays) (Wildes *et al.*, 1997), beam steering, synthetic apertures, 2D and sparse arrays, configurable arrays, parallel beamforming, micro-beamformers, rectilinear scanning, coded excitation, phased subarray processing, phase aberration correction, and others (Drinkwater, Wilcox, 2006; Johnson *et al.*, 2005; Karaman *et al.*, 2009; Kim, Song, 2006; Lockwood, Foster, 1996; Nowicki *et al.*, 2009). The most common complication introduced by these methods is a significant increase in channel count. Generating narrow ultrasonic wave

beams in biological media by multielement probes, built as matrices of elementary piezoceramic transducers in a rectangular configuration, can be realised by using transducers having spherical surfaces, ultrasonic lenses, mechanical elements (e.g. a complex system of properly rotated prisms), focusing devices or electronic devices, which control the system of activating and powering individual matrix elements in a proper manner (Drinkwater, Wilcox, 2006; Ermert *et al.*, 2000; Granz, Oppelt, 1987; Green *et al.*, 1974; Nowicki, 1995; Opieliński, Gudra, 2009; Opieliński *et al.*, 2009; 2010; Ramm, Smith, 1983; Thomenius, 1996).

Exciting individual transducers of the multielement probe using pulses with various delay is a universal method of focusing and deflecting a beam (Johnson *et al.*, 2005; Thomenius, 1996). Adequate delays between activations of each successive elementary transducer allow shaping of the wavefront and the direction of its propagation. The total delay Δt required to deflect a beam through angle of θ and to achieve a beam focus depth of F, can be expressed by the following formula (Ramm, Smith, 1983):

$$\Delta t = \frac{F}{c}\left(1 - \sqrt{1 + \left(\frac{nd}{F}\right)^2 - 2\frac{nd}{F}\sin\theta}\right) + t_0, \tag{1}$$

where c – ultrasonic wave propagation velocity in a medium, d – the distance (pitch) between the centres of adjacent ultrasonic transducers of a linear probe, n – the number of elementary transducers in the activation sequence, t_0 – initial delay, required to compensate negative delays. If the value of delay between activation of each successive transducer grows linearly, the wave beam is deflected through $\theta = \arcsin((\Delta t \cdot c)/(n \cdot d))$ angle (Somer, 1969). If the delay between activation of each successive transducer of the linear probe changes as a parabolic function of time, it will result in focusing of the beam (Fig. 1). This method of focusing is the most popular in case of linear USG probes.

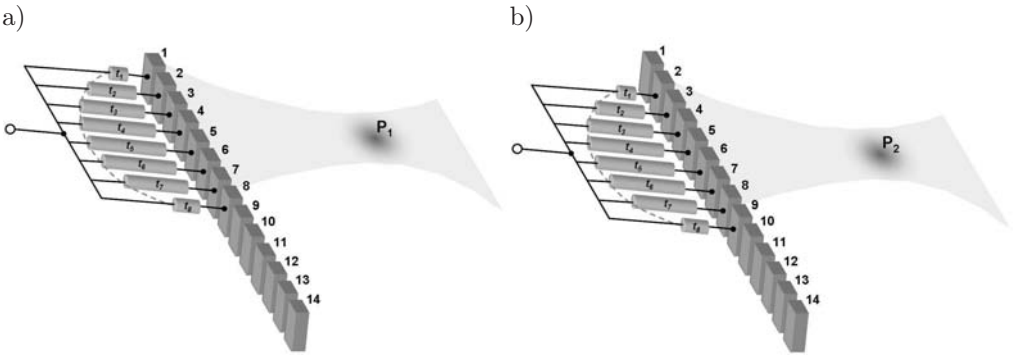

Fig. 1. The method of focusing a beam of a linear multielement probe by delaying activation of elementary transducers according to a parabolic function for sector $n = 8$: a) activation of the first sector, b) activation of the second sector.

In the example shown in Fig. 1, transducers 1 and 8 of the linear multielement ultrasonic probe are excited first. Next, transducers 2 and 7 are activated, followed by 3 and 6. Finally, transducers 4 and 5 are activated. The delay between the activations is determined so that the resultant wave focuses at P_1 (Fig. 1a). This is followed by similar activation of a sequence of pairs of 8 transducers 2–9, which generate ultrasonic wave beam focused at P_2 (Fig. 1b), etc. The reception of the reflected waves occurs in reverse order in the linear USG probe. The wave reflected at point P reaches individual probe transducers at various instants of time. If the time variations are balanced, phases of all waves will be in accordance and the resultant signal will be amplified. The typical linear USG probes are constructed from 64 or 128 transducers, which allows generation of a sequence of 57 or 121 independent beams shifted in relation to each other by the distance d equal to the distance (pitch) between the centres of adjacent transducers (Nowicki, 1995). Figure 2 shows the relation, calculated on the basis of formula (1), of the total delay Δt required to focus a beam in tissue with the focusing depth of $F = 3$ cm to distance d between the transducers of a linear probe, where the parameters of the number of transducers in a sequence focusing in succession $n = 2, 3, ..., 8$, $\theta = 0°$, $c = 1500$ m/s, $t_0 = 40$ μs were assumed for the calculations.

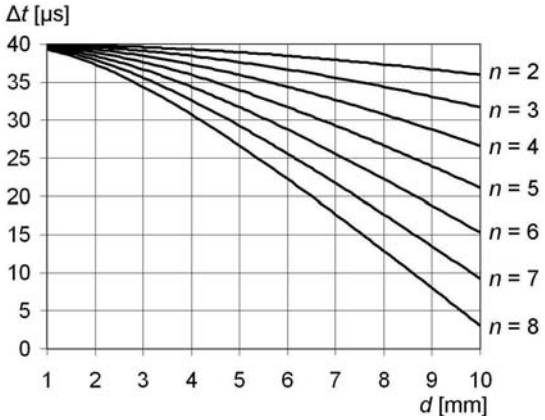

Fig. 2. The relation, calculated using formula (1), of the total delay required to focus a beam in tissue with the focusing depth of $F = 3$ cm, in function of the distance d between the centres of adjacent transducers (pitch) of a linear probe for focusing sequences $n = 2, 3, ..., 8$.

Calculations show that delay times between activation of each successive transducer of the linear probe shaped on the basis of spherical function of time, can be similar or shorter than pulse duration (e.g. for $f = 2$ MHz and length of 10 cycles of the burst pulse, its duration is 5 μs), which makes it necessary to use a separate generator with regulated delay in the sending system of each transducer of the focusing section. In case of multielement ultrasonic matrices (Opieliński, Gudra, 2009; Opieliński *et al.*, 2010) used for projection imaging of internal structure of biological media (transmission method, as in case of roentgenography

(Ermert *et al.*, 2000; Granz, Oppelt, 1987; Green *et al.*, 1974; Opieliński, Gudra, 2005; Parmar, Kolios, 2006)), introduction of delays of propagation of pulse ultrasonic wave for individual transducers can result in imaging the errors associated with side lobes. This method of focusing makes it also necessary to develop synchronised delaying systems and sophisticated technologies of attaching a large number of electrodes to the surface of minute piezoceramic transducers, by integration of some of the electronics with the transducer array enabling miniaturization of the front-end and funneling the electrical connections of a 2D array consisting of hundreds of elements into a reduced number of channels (Eames, Hossack, 2008; Opieliński, Gudra, 2009; Opieliński *et al.*, 2010; Wygant, Karaman *et al.*, 2006; Wygant, Lee *et al.*, 2006; Yen, Smith, 2004).

The experimental results have shown that using double ultrasonic pulse transmission of short coded sequences based on well-known Golay complementary codes, allows considerably to suppress the noise level (Drinkwater, Wilcox, 2006; Trots *et al.*, 2008). However, this type of transmission is more time-consuming.

Increase of directivity and intensity of the wave generated by the multielement ultrasonic probe can be achieved by simultaneous in-phase powering (no delays) of sequences of many elementary transducers (using one generator) in the sending system (which will however result in the probe's input impedance decrease), or by simultaneous receiving of the ultrasonic wave by means of sequences of many elementary transducers (Chiao, Thomas, 1996; Hoctor, Kassam, 1990; Karaman *et al.*, 2009; Lockwood, Foster, 1996; Trots *et al.*, 2009; Wygant, Karaman *et al.*, 2006; Yen, Smith, 2004). Such sending probes are usually activated by low-power generators of sinusoidal burst-type pulses, the generated voltage values of which are low (a couple of tens of volts peak-to-peak) and output resistance of about 50 Ω. If the probe's impedance is close to output impedance of the generator, it results in a decrease of amplitude of activating pulse voltage, which in turn causes decrease of intensity of the ultrasonic wave generated in the medium. Figure 3 shows examples of calculations of acoustic field distribution for a 16-element piezoceramic transducer matrix in a 4×4 array at various distances to the matrix with one, two, three and all of its columns being activated in succession. In the far field, on a plane which is perpendicular to the Z axis, distribution of the field generated by multielement probes with simultaneous activation of a group of elementary transducers has successive maximums and minimums (Fig. 3). The position of the maximums and minimums and amplitude of the main lobe and side lobes depends on dimensions of the probe's elementary transducers, the distance between them and the length of the wave radiated into the medium. The main lobe occurs for angle $\theta = \varphi = 0^\circ$, along the axis of symmetry of the active matrix elements. The other maximums occur for angles $\theta = \arcsin(n_x \cdot \lambda/d)$ and $\varphi = \arcsin(n_y \cdot \lambda/d)$, where n_x and n_y indicate the number of active transducers in horizontal and vertical plane of the matrix respectively. If the distance between adjacent transducers is small

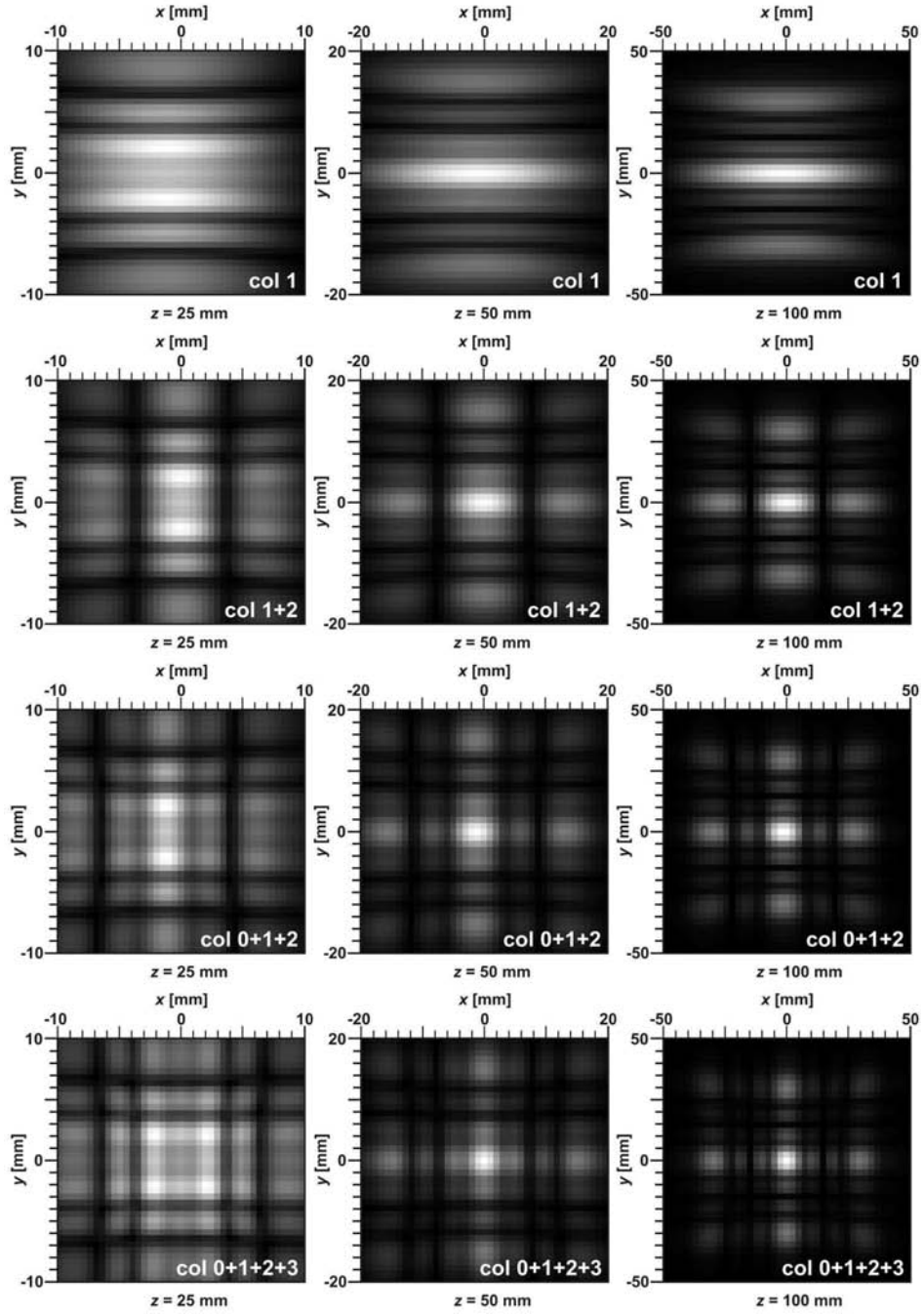

Fig. 3. Simulation of acoustic field distributions for a 16-element piezoceramic transducer matrix (size: 1.6 × 1.6 mm, $d = 2.5$ mm, $f = 2$ MHz) in a 4 × 4 array at distances of $z = 25$, 50 and 100 mm, with one, two, three and four of its columns being activated in succession (distribution geometrical centre overlaps with the matrix centre).

enough ($d < \lambda/2$), there are no side lobes in 90° sector. However, it is difficult to satisfy this criterion because for 2 MHz frequency, the wave length in tissue is about 0.75 mm, which necessitates the use of elementary transducers smaller than 0.375 mm.

However, there are various mechanisms that suppress grating side lobes (a few wavelengths short excitation pulses, apodization weighting functions, a different transmit and receive geometries, random element spacing) and hence allow this criterion to be somewhat relaxed in practice (Drinkwater, Wilcox, 2006; Karaman *et al.*, 2009; Kim, Song, 2006; Lockwood, Foster, 1996; Thomenius, 1996; Yen, Smith, 2004).

Recently in the medical imaging field, a number of authors have suggested the use of arrays with large numbers of elements and investigated methods of selecting the optimal numbers and distribution of elements for the transmit and receive apertures (Drinkwater, Wilcox, 2006). The development of 2D arrays for clinical ultrasound imaging could greatly improve the detection of small or low contrast structures. Using a 2D array, the ultrasound beam could be symmetrically focused and scanned throughout a volume (Lockwood, Foster, 1996; Yen, Smith, 2004). The majority of 2D ultrasonic multielement matrices are designed for miniature 3D volumetric medical endoscopic imaging as intracavital probes, provided unique opportunities for guiding surgeries or minimally invasive therapeutic procedures (Eames, Hossack, 2008; Karaman *et al.*, 2009; Wygant, Karaman *et al.*, 2006; Wygant, Lee *et al.*, 2006). It can be concluded, basing on worldwide literature review, that most of the 2D ultrasonic arrays is assigned to work of the echo method (Drinkwater, Wilcox, 2006); there are not so many developments of 2D matrices designed for ultrasonic projection imaging (transmission method) (Ermert *et al.*, 2000; Granz, Oppelt, 1987; Green *et al.*, 1974; Opieliński, Gudra, 2005; Parmar, Kolios, 2006; Opieliński, Gudra, 2009; Opieliński *et al.*, 2009; Opieliński *et al.*, 2010). This paper presents an idea of minimising the number of connections between individual piezoelectric transducers in a row-column multielement passive ultrasonic matrix system, used for imaging of biological media structure by means of ultrasonic projection (Opieliński, Gudra, 2005). It allows to achieve significant directivity and increased wave intensity with acceptable matrix input impedance decrease. This concept was verified by designing a model of a passive matrix consisting of 16 elementary ultrasonic transducers, with electrode attachments optimised by means of electronic switches in rows and columns.

2. Activation method

Passive matrix is the simplest matrix control solution. There are two groups of switches in this type of matrix, one for a selected active column and the other for a selected active row. The transducer situated at the point of intersection of

the selected row and column is activated in this way (Fig. 4a). The piezoceramic transducers of the matrix are powered with a high frequency (a couple of MHz) alternating signal. In the context of an electric circuit, the construction of the transducers (dielectrics with sprayed-on electrodes) means that they are capacitive in nature and that therefore, the activating signal can travel through inactive transducers to other column and row lines, despite their switches being opened (Fig. 4b).

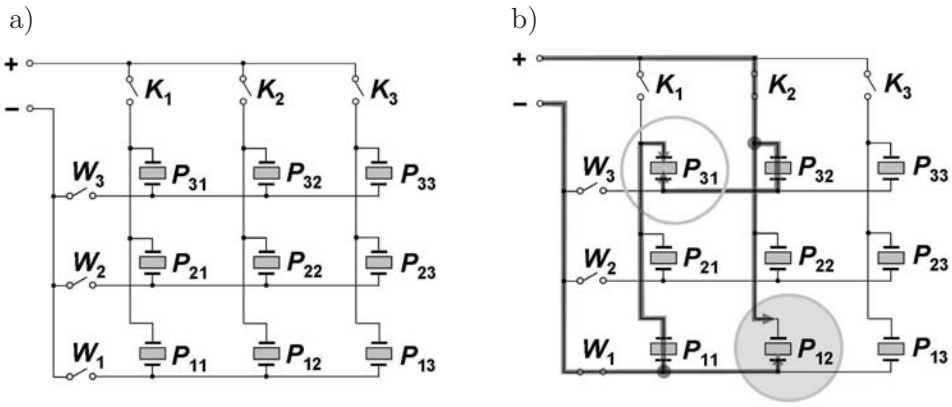

Fig. 4. Diagram of transducer connections in a passive matrix (a) and crosstalk occurrence (b).

The directivity and effectiveness/sensitivity of such a probe will thus largely depend on the distribution pattern of the activating signal voltages on all elementary transducers of the matrix, which are excited in this manner (with crosstalks) (Opieliński *et al.*, 2009; Opieliński *et al.*, 2010).

3. Matrix design

In order to construct a model of a passive ultrasonic matrix, a suitable PCB (printed circuit board) was designed and produced. It was utilized as an elementary transducer pad in a 4×4 array (Fig. 5). Piezoceramic plates were mounted

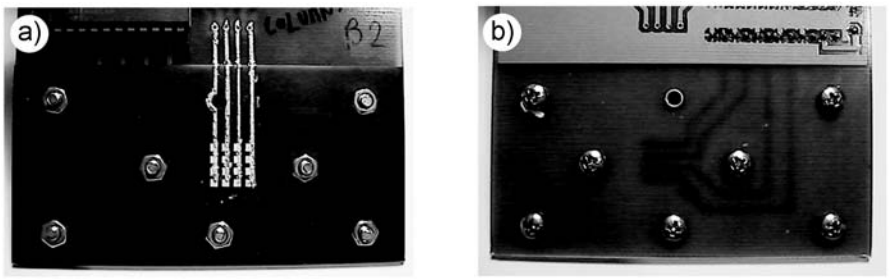

Fig. 5. Part of the designed ultrasonic matrix: a) front, b) back.

using a designed and produced engraving laminate mesh with laser-cut openings (openings – 1.6×1.6 mm, distance between the openings – 0.9 mm). Pz37 Ferroperm piezoceramics plates, $1.6 \times 1.6 \times 0.9$ mm, in the mounting mesh, were attached to PCB traces (rows) using a small amount of conductive glue. Additionally, the mounting mesh was screwed to the PCB using bolts (Fig. 5).

MAX335 integrated circuits were used as switches. It is possible to transmit signals with up to 30 Vpp voltage value. Column traces were connected using silver conductive adhesive with suitable hardener (Fig. 5a). The area of the matrix that was to be submerged in water, was sprayed to achieve a transparent acrylic coating characterised by good insulation properties, which additionally functions as a matching layer. The area was later given additional transparent silicon rubber coating.

Amplitude-phase characteristics of 16 transducers selected for construction of the matrix model from a group of 280, on the basis of repeatability of the selected $f_r = 2.091$ MHz resonance frequency and $G(f_r)$ conductance value, show no f_r value dispersion at frequency measurement resolution of 4.01 kHz and dispersion of $\Delta G(f_r) \approx 400$ µS and $\Delta B(f_r) \approx 300$ µS, with measurement uncertainty of 0.05% (Fig. 6).

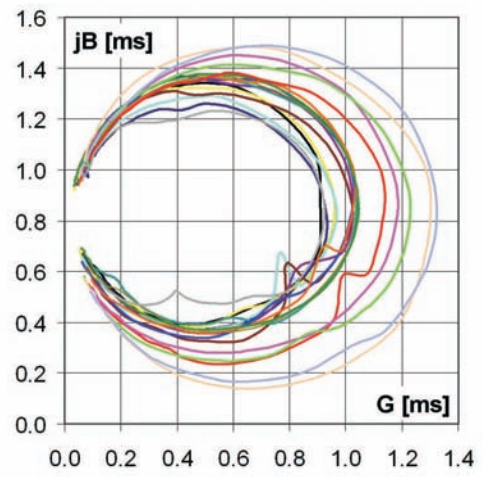

Fig. 6. Amplitude-phase characteristics of 16 selected elementary transducers for frequency range of 2.00–2.16 MHz.

4. Measurements and calculations

Figure 7 shows $G(f)$ and $B(f)$ relations and amplitude-phase characteristics $(G + jB)$ for all elementary transducers of the designed model of a passive matrix submerged in water, which were measured on the receiving side using a HP

3589A network analyser, after every transducer had been activated individually with a suitable electronic switch (Fig. 4). In the frequency range of 1.4–2.4 MHz, elementary transducers of the model of a passive matrix can operate at 3 resonant frequencies: $f_{r1} \approx 1.6$ MHz, $f_{r2} \approx 1.8$ MHz and $f_{r3} \approx 2$ MHz. However, they are all in a broad band of $\Delta f \approx 1.55$–2.2 MHz (Fig. 7), for which, as it can be assumed, the average resonant frequency is $f_{r\_av} \approx 1.84$ MHz (quality factor: $Q = 2.8$). All three partial resonances in this band are characterised by the Q factor of $Q \approx 10$. The spread of resonance frequency values is small, while the spread of the corresponding conductance values is in the range of $\Delta G \approx 0.3$–0.5 mS.

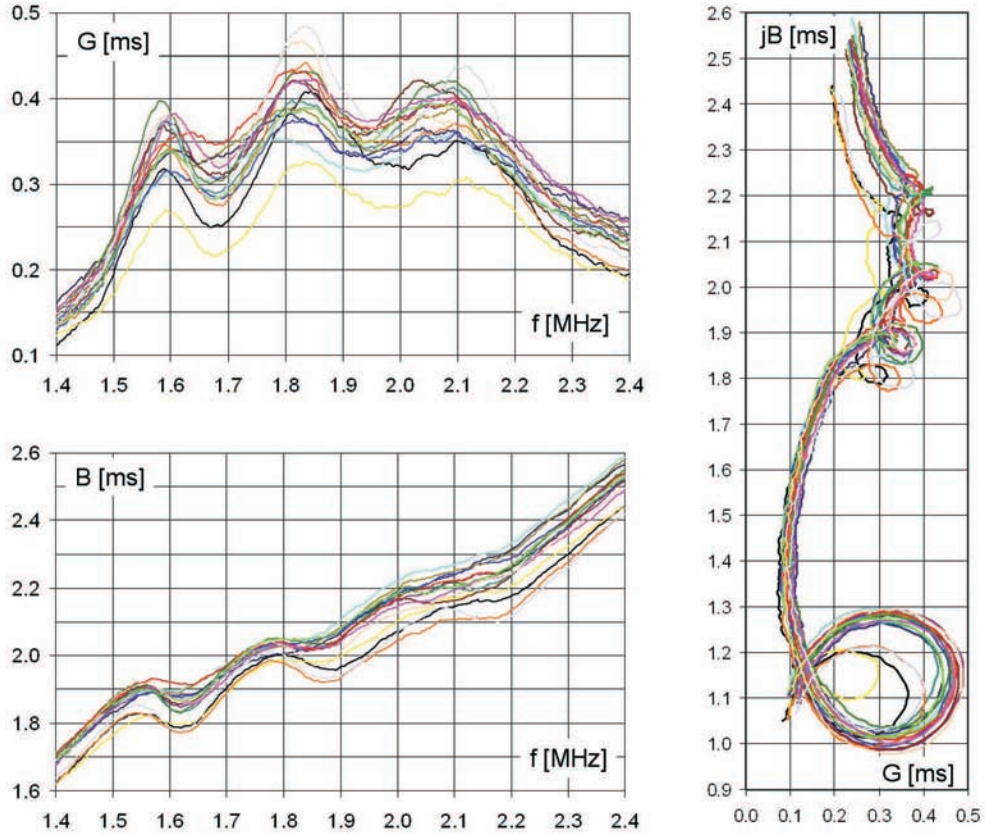

Fig. 7. Conductance $G(f)$, susceptance $B(f)$ in 1.4–2.4 MHz frequency range and amplitude-phase characteristics of 16 elementary transducers of the developed model of a passive matrix, in the 0.8–2.4 MHz frequency range.

Imaginary part of amplitude-phase characteristics of passive matrix transducers (Fig. 7) points to their capacitive nature ($C_o \approx 160$ pF, in which connection cables capacitance is about 100 pF, $R_o \approx 3$ kΩ, $|Z(f_r)| \approx 2$ kΩ). Individual transducers of multielement probes, which were designed earlier, with separated

electrode attachments (classic matrix) showed capacitance of $C_o \approx 10$ pF, resistance of electric losses $R_o \approx 30$ kΩ and impedance in resonance: $|Z(f_r)| \approx 7$ kΩ (Opieliński, Gudra, 2009) (for comparison: if all 16 transducers of the matrix were activated using the same voltage U, the system impedance would be $|Z(f_r)| \approx 440$ Ω). These values suggest that in case of a passive matrix there is a phenomenon of increasing transducers' capacitance and reducing their resistance, resulting from parallel connection of all the elements of the matrix. This in turn confirms occurrence of crosstalks in such a system (Fig. 4b). Calculations and measurements of voltages show that after the electrodes are connected to a given row and column of the model of a passive matrix (Fig. 4), the transducer at the point of intersection of that row and column will be activated by the supplied voltage U; all the other transducers in this row and column will be activated by voltage of $0.4U$ and the rest of the transducers of the matrix will be activated by voltage of $-0.15U$ (Fig. 8). This phenomenon seems advantageous in the context of achieving a directional beam of ultrasonic wave and reducing the matrix input impedance.

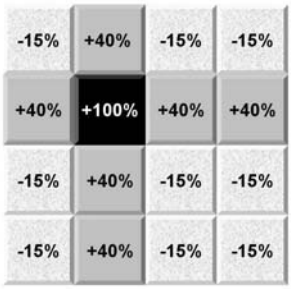

Fig. 8. Image of crosstalks in the model of a passive matrix, after activation of a transducer in the second column from the left and third row looking from the bottom.

Hydroacoustic measurements of the constructed transducer matrix model were performed using a set-up presented in Fig. 9.

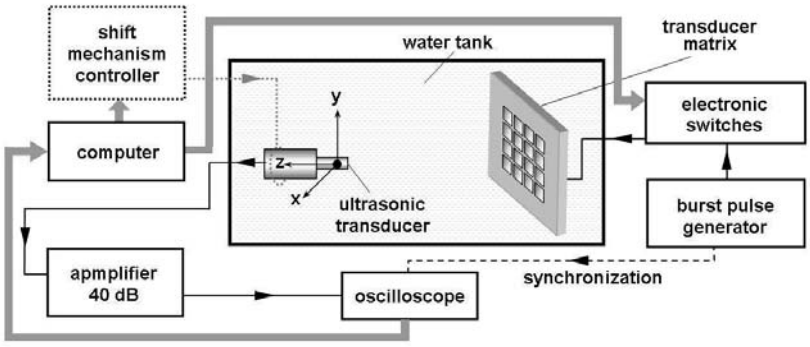

Fig. 9. A block diagram of the set-up for automatic measurement of 3D acoustic field distribution for a model of a passive matrix.

The transducers of the matrix were activated with burst pulses with repetition frequency of $f_p = 100$ Hz, filled with a sinusoidal signal of frequency $f = 2.09$ MHz and length of 10 cycles. The pulse amplitude was 20 Vpp. Acoustic field generated by the probe's elementary transducers was measured in water, on a plane that was parallel to the surface of the matrix (perpendicular to the direction of propagation), at the distances of 25 and 50 mm from the probe's surface, in the area of 20×20 mm (geometrical area centre in the receiving probe axis). The receiving probe, the diameter of which was 5 mm and operating frequency was $f_r = 5$ MHz, was situated centrally in relation to the surface of the matrix as it is seen in Fig. 10. Then by electronically activating individual transducers of the matrix (No. 3.0, 3.1, 2.0, 2.1), the computer controlled set-up measured acoustic field (Fig. 11, Fig. 12) automatically moving (by means of step motors) a receiving probe in the area of 20×20 mm, with a 0.5 mm step. The receiving probe was characterised by the highest sensitivity and smallest diameter among all ultrasonic transducers available to the team, that operate at the frequency range of $f = 1$–5 MHz. Due to limited spatial resolution of the measurement probe (smoothing of field distribution) and its determined directivity (minimisation of values outside axis), the pseudo-3D acoustic field distributions $U(x, y)$ measured by means of an oscilloscope were additionally imaged with limited dynamics $U_{LD}(x, y) = (20 \cdot \log(U(x, y)) - A_1) \cdot A_2$; this allowed observation of small values $U(x, y) \sim p(x, y)$ (Fig. 11, Fig. 12). The A_1 and A_2 coefficient was specially selected in order to level out maximum and minimum measurement values $U_{LD}(x, y)$ with calculation values $p(x, y)$ for every distribution.

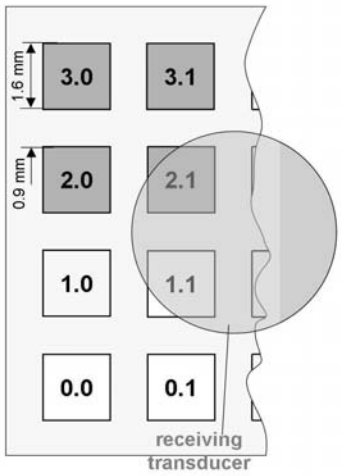

Fig. 10. Marked position of the receiving probe in relation to the surface of the matrix and marked measured elements of the matrix.

The calculations of acoustic field distribution of the designed passive matrix submerged in water (Fig. 11, Fig. 12) were performed using the method of nu-

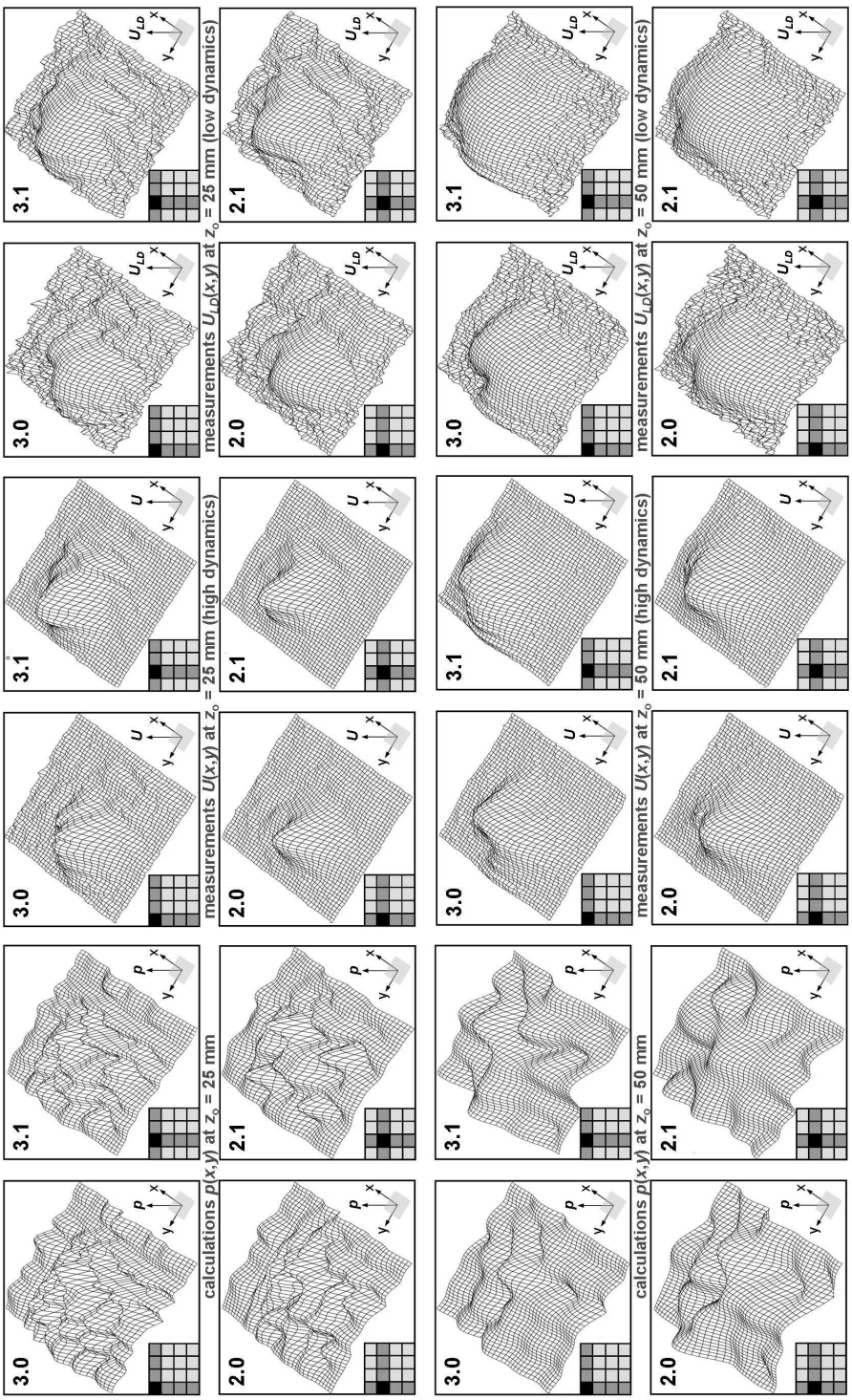

Fig. 11. Comparison of measurements of acoustic field distribution of the designed model of a passive matrix, with calculations in the form of pseudo-3D graphs.

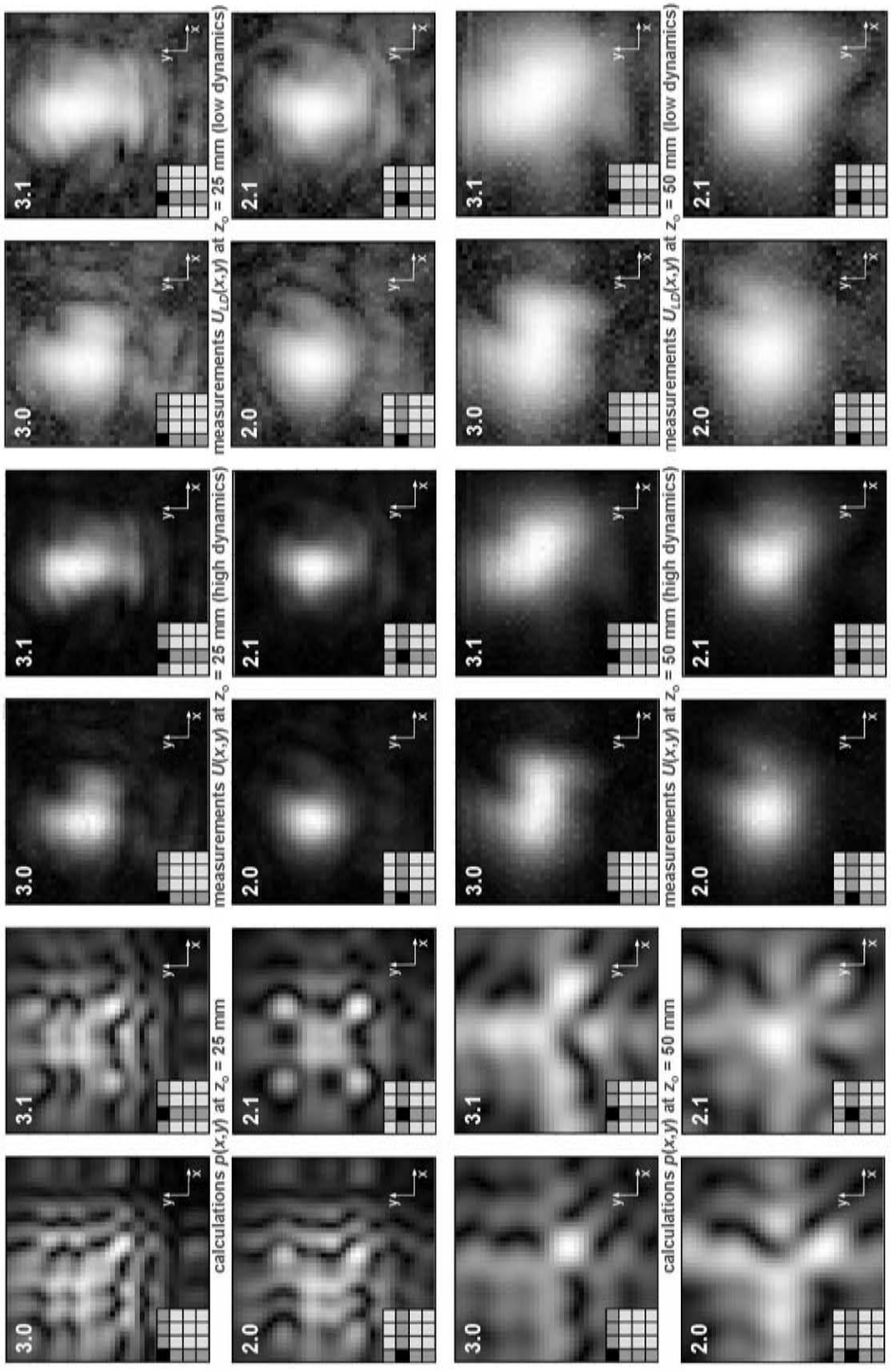

Fig. 12. Comparison of measurements of acoustic field distribution of the designed model of a passive matrix, with calculations in the form of greyscale contour graphs.

merically summing the fields of the elementary transducers shaped as squares, the sides of which were $a = 1.6$ mm (Opieliński, Gudra, 2006):

$$p = \left| \sum_{n=0}^{N-1} \sum_{m=0}^{M-1} -j \frac{\rho c k a^2}{2\pi R(m,n)} \cdot V_o(m,n) \cdot \left(\frac{\sin\left(\frac{ka \sin(\theta(n))}{2} \right)}{\frac{ka \sin(\theta(n))}{2}} \right) \right.$$
$$\left. \cdot \left(\frac{\sin\left(\frac{ka \sin(\varphi(m,n))}{2} \right)}{\frac{ka \sin(\varphi(m,n))}{2}} \right) \cdot e^{j(\omega t - kR(m,n))} \right|, \tag{2}$$

where p – acoustic pressure, ρ – water density, c – sound velocity in water, k – wave number, a – transducer's side length, M – number of matrix rows, N – number of matrix columns, $R(m,n)$, $\theta(m,n)$, $\varphi(m,n)$ – polar coordinates of the distribution point modified in relation to the position of the transducer in the matrix, $V_o(m,n)$ – acoustic velocity for a matrix transducer. Graphic illustration of the calculation algorithm is shown in Fig. 13.

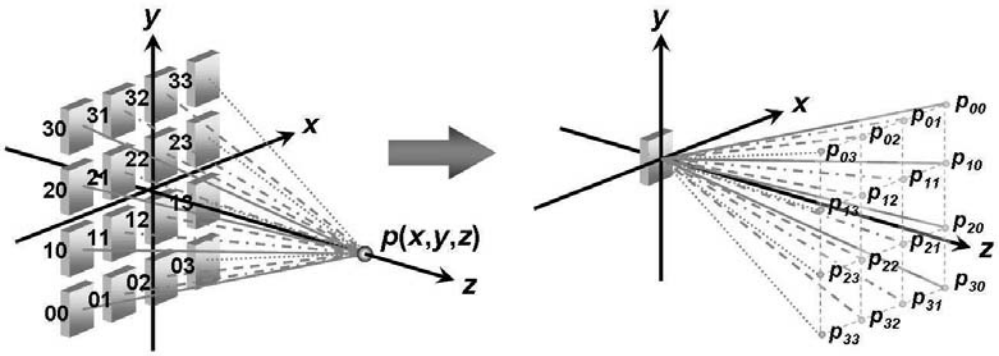

Fig. 13. Graphic illustration of the developed algorithm for calculation of acoustic field distribution for flat matrices of ultrasonic transducers.

Value of acoustic pressure $p(x,y,z)$ for all active elements of the matrix is calculated as a sum of pressure values p_{mn} for a single element in many points of the medium with specified acoustic velocity value $V_o(m,n)$. If the orientation of matrix in the coordinate system is as shown in Fig. 13, the following formulas are valid:

$$r(n) = \sqrt{x(n)^2 + z^2}, \tag{3}$$

$$R(m,n) = \sqrt{r(n)^2 + y(m)^2} = \sqrt{x(n)^2 + y(m)^2 + z^2}, \tag{4}$$

$$\sin\theta(n) = \frac{x(n)}{r(n)} = \frac{x(n)}{\sqrt{x(n)^2 + z^2}}, \tag{5}$$

$$\sin\varphi(m,n) = \frac{y(m)}{R(m,n)} = \frac{y(m)}{\sqrt{x(n)^2 + y(m)^2 + z^2}}. \tag{6}$$

If we adopt designations for individual transducers as shown in Fig. 13 for the number of rows $m = 0, 1, 2, ..., M-1$ and columns of the matrix $n = 0, 1, 2, ..., N-1$, it is possible to define the modified coordinates $x(n)$ and $y(m)$ in the following way:

$$x(n) = x + (N - 1 - 2 \cdot n) \cdot \frac{d}{2}, \tag{7}$$

$$y(m) = y + (M - 1 - 2 \cdot m) \cdot \frac{d}{2}. \tag{8}$$

Modification of x and y coordinates results from the fact that it is necessary to virtually shift the field distribution point $P(x, y, z)$ to coordinates $P'(x(n), y(m), z)$ in such a manner, that it would be possible to sum the complex values of acoustic pressure generated by each elementary transducers of the matrix (for which acoustic velocity is specified by value $V_o(m, n)$) at point $P(x, y, z)$. Acoustic field generated by the probe's elementary transducers (transducer activated by the applied voltage U, all other transducers in this row and column activated by voltage $0.4U$, the rest of the transducers of the matrix activated by voltage $-0.15U$) was simulated using formula (2) in water, on XY plane parallel to the surface of the matrix (perpendicular to the direction of propagation) at the distance of $z = 25$ and 50 mm from the surface of the matrix, in the area $x \times y = 20 \times 20$ mm (geometrical centre of the area overlaps with the centre of the matrix) (Fig. 11, Fig. 12). The following parameters were assumed for all the calculations: $\rho_o = 1000$ kg/m^3, $c = 1490$ m/s, $f_r = 2$ MHz, $a = 1.6$ mm, $d = 2.5$ mm, $M = N = 4$, $V_o(i) \sim U(i)$ (for the activated transducer it was assumed that $V_o = 0.1$ m/s).

Figure 14 presents a comparison between the calculations and measurements of acoustic field distribution along the Y axis ($x = 0$) for the designed model of a passive matrix and for a classic matrix, with no crosstalk (activated transducer No. 2.1) at the distance of $z = 50$ mm from the surface of the matrix.

Measurements and calculations indicate that the designed model of a passive matrix allows to achieve significantly higher directivity and amplitude of ultrasonic wave generated in a media than that in case of powering a single, electrically separated transducer of a classic matrix (Fig. 11, Fig. 12, Fig. 14, Fig. 15). The divergence angle of the beam generated by the designed model of a passive matrix when one element is activated, is about 6–8° (Fig. 14, Fig. 15).

In case of separate activating of individual transducers of the model of a passive matrix, despite the crosstalk, correct shift of the maximum of the received signal is clearly seen, which in case of projection imaging of the structure of

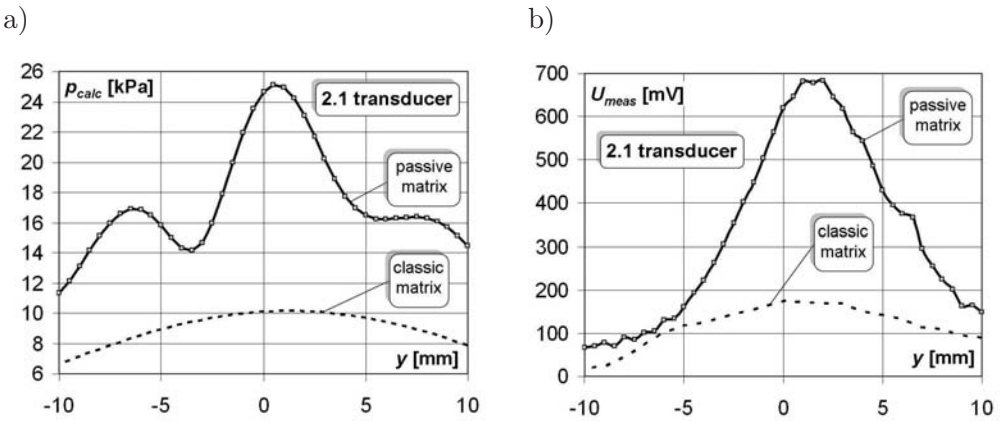

Fig. 14. A comparison between the calculations (a) and measurements (b) of acoustic field distribution along the Y axis ($x = 0$), for the designed model of a passive matrix and for a classic matrix with no crosstalk at the distance of $z = 50$ mm from the surface of the matrix (activated transducer No. 2.1).

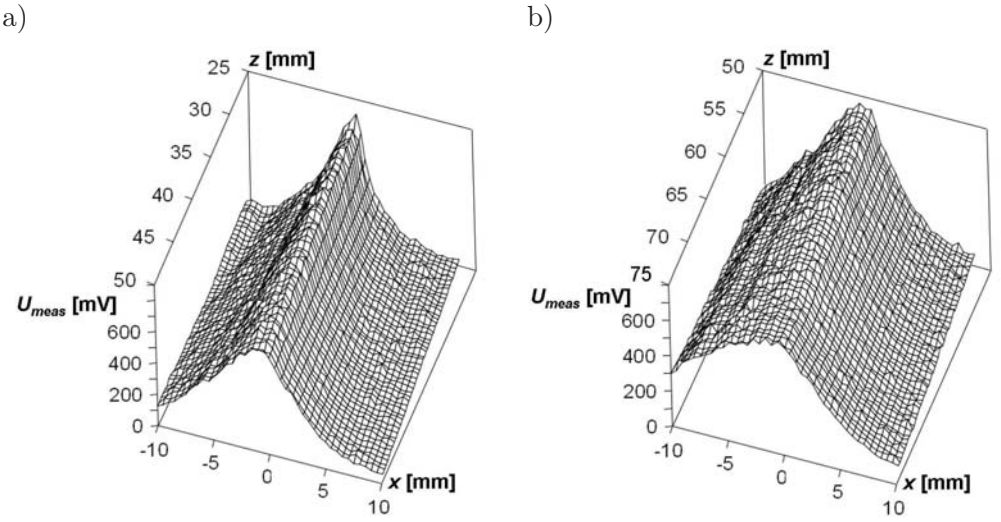

Fig. 15. Pseudo-3D distributions of acoustic field measured for the designed model of a passive matrix in a plane parallel to the direction of ultrasonic wave propagation in the axis of the matrix ($y = 0$, activated transducer No. 2.1): a) area $x = -10$–10 mm, distance from the matrix $z = 25$–50 mm, b) area $x = -10$–10 mm, distance from the matrix $z = 50$–75 mm.

biological media enables scanning in orthogonal projection (Fig. 11, Fig. 12). Calculations show incoherence of distribution of acoustic field generated by activated transducers of the passive matrix, especially in near field, which for the designed 16-element model is about 25 mm (Fig. 16). Measurements with 5 mm diameter ultrasonic probe showed however, that there are coherent maximums of field distribution, which are the result of averaging on the surface of the receiving transducer.

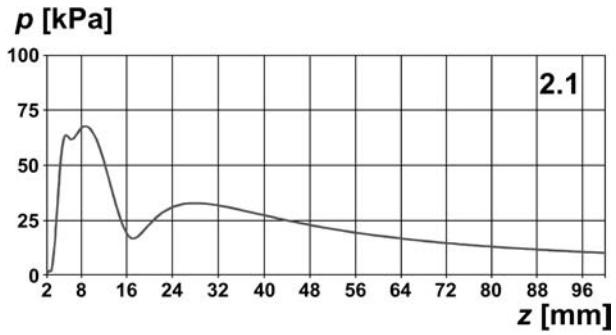

Fig. 16. Modulus of acoustic pressure distribution $p(z)$ determined numerically, using formula (2) for the designed model of a passive ultrasonic matrix, along its axis of symmetry (activated transducer No. 2.1).

5. Conclusions

Calculation and measurement results of acoustic field distributions conform well, which means that the prepared algorithm can be used to determine acoustic field distributions of flat matrices of elementary piezoceramic transducers in a rectangular configuration. The slight differences result from the averaging character of the used receiving probe and possible unparallel surfaces and varying effectiveness of elementary transducers.

Calculations and measurements of acoustic field distribution of the designed model of a passive matrix show that when one elementary transducer is activated, all other transducers of the matrix are also activated by voltages that fall into a specific pattern. As a result of this, the matrix generates a directional beam. Activating elementary transducers in a row-column multielement passive ultrasonic matrix system allows a significant minimisation of the number of connections of individual piezoelectric transducers. For example, for a 1024-element matrix it is sufficient to use 64 traces printed on a PCB and supplying signal-activating elementary transducers, instead of attaching 1024 separate electrodes in the form of thin insulated leads soldered to the surface of the transducers and mounting multi-pin connectors. The concept of a passive matrix allows to achieve high directivity and increased wave intensity with acceptable input impedance decrease.

Acknowledgments

This research was carried out as part of grant No. N N515 410634 funded by MNiSW (Ministry of Science and Higher Education of Poland) in the years 2008–2011.

This article is an extended version of the paper presented at the 56-th Open Seminar on Acoustics – OSA2009, September 15–18 in Goniądz.

References

1. Chiao R.Y., Thomas L.J. (1996), *Aperture formation on reduced-channel arrays using the transmit-receive apodization matrix*, 1996 IEEE Ultrasonics Symposium Proceedings, 1567–1571.
2. Drinkwater B.W., Wilcox P.D. (2006), *Ultrasonic arrays for non-destructive evaluation: A review*, NDT&E International, **39**, 525–541.
3. Eames M.D.C., Hossack J.A. (2008), *Fabrication and evaluation of fully-sampled, two-dimensional transducer array for "Sonic Window" imaging system*, Ultrasonics, **48**, 376–383.
4. Ermert H., Keitmann O., Oppelt R., Granz B., Pesavento A., Vester M., Tillig B., Sander V. (2000), *A New Concept for a Real-Time Ultrasound Transmission Camera*, 2000 IEEE Ultrasonics Symposium Proceedings, 1611–1614.
5. Granz B., Oppelt R. (1987), *A Two-Dimensional PVDF Transducer Matrix as a Receiver in an Ultrasonic Transmission Camera*, Acoustical Imaging, **15**, Plenum Press, New York, 213–225.
6. Green P.S., Schaefer L.F., Jones E.D., Suarez J.R. (1974), *A New High Performance Ultrasonic Camera*, Acoustical Holography, **5**, Plenum Press, New York, 493–503.
7. Hoctor R.T., Kassam S.A. (1990), *The Unifying Role of the Coarray in Aperture Synthesis for Coherent and Incoherent Imaging*, Proceedings of the IEEE, **78**, 4, 735–752.
8. Johnson J.A., Karaman M., Khuri–Yakub B.T. (2005), *Coherent-Array Imaging Using Phased Subarrays. Part I: Basic Principles*, IEEE Transactions on Ultrasonics, Ferroelectrics, and Frequency Control, **52**, 1, 37–50.
9. Karaman M., Wygant I.O., Oralkan Ö., Khuri–Yakub B.T. (2009), *Minimally Redundant 2-D Array Design for 3-D Medical Ultrasound Imaging*, IEEE Transactions on Medical Imaging, **28**, 7, 1051–1061.
10. Kim J-J., Song T-K. (2006), *Real-Time High-Resolution 3D Imaging Method Using 2D Phased Arrays Based on Sparse Synthetic Focusing Technique*, 2006 IEEE Ultrasonics Symposium Proceedings, 1995–1998.
11. Lockwood G.R., Foster F.S. (1996), *Optimizing the Radiation Pattern of Sparse Periodic Two-Dimensional Arrays*, IEEE Transactions on Ultrasonics, Ferroelectrics, and Frequency Control, **43**, 1, 15–19.
12. Nowicki A. (1995), *Basis of Doppler Ultrasonography* [in Polish], PWN, Warszawa.
13. Nowicki A., Wójcik J., Kujawska T. (2009), *Nonlinearly Coded Signals for Harmonic Imaging*, Archives of Acoustics, **34**, 1, 63–74.
14. Opielinski K.J., Gudra T. (2005), *Computer recognition of biological objects' internal structure using ultrasonic projection*, Computer Recognition Systems (Advances in Soft Computing), Berlin, Springer, 645–652.
15. Opieliński K.J., Gudra T. (2006), *Determining the acoustic field distribution of ultrasonic multi-element probes*, Archives of Acoustics, **31**, 4, 391–396.
16. Opielinski K.J., Gudra T. (2009), *Multielement ultrasonic probes for projection imaging*, Proceedings of the International Congress on Ultrasonics, Santiago de Chile, January 11–17 2009, Physics Procedia (in print).

17. Opieliński K.J., Gudra T., Pruchnicki P. (2009), *The method of a medium internal structure imaging and the device for a medium internal structure imaging* [in Polish], Patent Application No. P389014 to the Patent Office of the Republic of Poland, Wrocław University of Technology.

18. Opieliński K.J., Gudra T., Pruchnicki P. (2010), *A Digitally Controlled Model of an Active Ultrasonic Transducer Matrix for Projection Imaging of Biological Media*, Archives of Acoustics, **35**, 1, 75–90.

19. Parmar N., Kolios M.C. (2006), *An investigation of the use of transmission ultrasound to measure acoustic attenuation changes in thermal therapy*, Med. Bio. Eng. Comput., **44**, 583–591.

20. Ramm von, O.T., Smith S.W. (1983), *Beam steering with linear arrays*, IEEE Trans. Biomed. Eng., **BME-30**, 8, 438–452.

21. Somer J.C. (1969), *Electronic sector scanning with ultrasonic beams*, Proceedings of the 1st World Congress on Ultrasound Diagnostics in Medicine, Vienna, 27.

22. Trots I., Nowicki A., Lewandowski M., Secomski W., Litniewski J. (2008), *Double pulse transmission – signal-to-noise ratio improvement in ultrasound imaging*, Archives of Acoustics, **33**, 4, 593–601.

23. Trots I., Nowicki A., Lewandowski M. (2009), *Synthetic Transmit Aperture in Ultrasound Imaging*, Archives of Acoustics, **34**, 4, 685–695.

24. Thomenius K.E. (1996), *Evolution of ultrasound beamformers*, 1996 IEEE Ultrasonics Symposium Proceedings, 1615–1622.

25. Wildes D.G., Chiao R.Y., Daft Ch.M.W., Rigby K.W., Smith L.S., Thomenius K.E. (1997), *Elevation performance of 1.25D and 1.5D Transducer Arrays*, IEEE Transactions on Ultrasonics, Ferroelectrics, and Frequency Control, **44**, 5, 1027–1037.

26. Wygant I.O., Karaman M., Oralkan Ö., Khuri–Yakub B.T. (2006), *Beamforming and hardware design for a multichannel front-end integrated circuit for real-time 3D catheter-based ultrasonic imaging*, SPIE Medical Imaging, **6147**, 61470A-1-8.

27. Wygant I.O., Lee H., Nikoozadeh A., Yeh D.T., Oralkan Ö., Karaman M., Khuri–Yakub B.T. (2006), *An Integrated Circuit with Transmit Beamforming and Parallel Receive Channels for Real-Time Three-Dimensional Ultrasound Imaging*, 2006 IEEE Ultrasonics Symposium Proceedings, 2186–2189.

28. Yen J.T., Smith S.W. (2004), *Real-Time Rectilinear 3-D Ultrasound Using Receive Mode Multiplexing*, IEEE Transactions on Ultrasonics, Ferroelectrics, and Frequency Control, **51**, 2, 216–226.